Lattice dynamics and Raman spectra of isotopically mixed diamond

K. C. Hass and M. A. Tamor
Ford Motor Company, SRL/MD3028, Dearborn, Michigan 48121-2053

T. R. Anthony and W. F. Banholzer
GE Corporate Research and Development, Building K1, Room 5A59, Schenectady, New York 12301
(Received 10 October 1991)

We present coherent-potential-approximation (CPA) calculations and first- and second-order Raman spectra for diamonds with varying concentrations of ^{12}C and ^{13}C. The calculations are based on the valence-force model of Tubino, Piseri, and Zerbi [J. Chem. Phys. **56**, 1022 (1972)]. Contrary to previous claims, we find that this model does not give a sharp peak in the density of states (DOS) near the Raman mode. Alternative dispersion curves that do give such a peak are discussed. Raman results are reported for high-quality, single-crystal synthetic diamonds with isotopic compositions ranging from nearly pure ^{12}C to nearly pure ^{13}C. A measurable deviation in the Raman frequency away from a simple $M^{-1/2}$ ("virtual-crystal") dependence and an observable broadening of the first- and second-order spectra are qualitatively consistent with CPA predictions for the effects of isotopic disorder. Quantitative agreement between theory and experiment is achieved only if the reference DOS contains the above-mentioned peak. This supports the interpretation of the controversial second-order Raman peak in naturally abundant diamond (1.1 at. % ^{13}C) at 2667 cm^{-1} as a DOS effect. At all compositions, the effects of isotopic disorder are relatively weak because of the small mass difference between ^{12}C and ^{13}C. For 1.1 at. % ^{13}C, the maximum broadening predicted in the CPA is less than 1 cm^{-1}, nearly two orders of magnitude smaller than a previous estimate. For the lowest-frequency modes most relevant to the thermal conductivity, the CPA scattering rate reduces to the usual ω^4 dependence first derived by Klemens for phonon-isotope scattering. Using Callaway's theory, we show that this term can easily account for the recently observed 50% enhancement in room-temperature thermal conductivity upon elimination of ^{13}C impurities, provided that sufficient normal scattering also occurs.

I. INTRODUCTION

Carbon has two stable isotopes, ^{12}C and ^{13}C, with natural abundances of 98.9 and 1.1 at. %, respectively. Natural diamond may thus be viewed as a random $A_{1-x}B_x$ crystalline alloy ($x=0.011$) in which the $A=^{12}C$ and $B=^{13}C$ constituents differ only in mass. Recently, workers at General Electric[1,2] (GE) have succeeded in growing large, high-quality single-crystal diamonds across the entire range of isotopic compositions from $x\approx 0$ to 1. The subsequent discovery[3] that the room-temperature thermal conductivity of nearly pure ^{12}C diamond ($x\approx 0.0007$) is over 50% greater than that of natural diamond has generated much scientific and technological interest. To understand this effect quantitatively, it is first necessary to understand how the phonon spectrum of diamond is affected by variations in isotopic composition. In a recent paper[4] (hereafter referred to as I), we began to address this issue with use of a combined theoretical and experimental approach based on the coherent-potential approximation[5-7] (CPA) and Raman spectroscopy. Here we give a more complete account of this work and discuss its implications for the thermal-conductivity behavior of diamond at low ^{13}C concentrations.

Studies of the vibrational and thermal properties of diamond have been of great historical importance in solid-state physics.[8] Implicit in almost all previous studies of these properties has been the assumption of an ordered crystal with identical atoms of average mass $\overline{M}$ ($=12.011$ amu for natural diamond). For most purposes this "virtual-crystal approximation" (VCA) is entirely adequate. In addition to being an excellent approximation for natural diamond, the VCA also describes the principal trend in phonon frequencies as the isotopic composition is varied: $\omega\propto\overline{M}^{-1/2}$.

The VCA does not include, however, any intrinsic broadening due to isotopic disorder. In a recent attempt to explain the thermal-conductivity enhancement in nearly pure ^{12}C diamond, Bray and Anthony[9] suggested that this broadening might be as large as 50 cm^{-1} in natural diamond. This estimate was based on an extremely crude model which gives only an upper bound on the broadening. More reliable methods for dealing with this classic problem of substitutional mass disorder are well known.[6] The present work is based on the phonon CPA of Taylor.[5] This method is expected to be extremely accurate for diamond since the scattering due to mass fluctuations is not very strong ($\Delta M/\overline{M}\ll 1$). The CPA formalism is computationally simple and involves no adjustable parameters once the VCA density of states (DOS) is specified. A previous application of this approach to isotopically mixed Ge has been described by Fuchs *et al.*[10] The present application to diamond is based on the valence-force parametrization of Tubino, Piseri, and Zerbi[11] (TPZ).

To test this approach, we compare our CPA results to measurements of the first- and second-order Raman spectra of high-quality, single-crystal, GE synthetic diamonds with varying ^{13}C concentrations. In I we showed that the frequency of the first-order Raman mode varies nonlinearly with composition and that its width varies asymmetrically, reaching a maximum at about 70 at. % ^{13}C. We further showed that both of these effects are qualitatively consistent with CPA calculations for the TPZ model; quantitatively, however, such calculations account for only about half of the observed broadening. This discrepancy was attributed in I to the failure of the TPZ model to give a peak in the DOS above the Raman mode. Tubino and Birman[12] has claimed that the TPZ model does give such a peak, but our results contradict this. The present work examines this point in more detail and concludes that a reliable VCA DOS for diamond should contain a peak above the Raman mode. CPA results obtained by artificially adding such a peak to the VCA DOS give much better agreement with the experimentally observed widths and shapes of the first-order Raman line. Such calculations are also consistent with measured second-order Raman spectra, which show a sharp peak near the top of the spectrum for dilute ^{12}C or ^{13}C concentrations,[13,14] but not in more concentrated "alloys." The origin of this second-order Raman peak in diamond has long been controversial.[12,15–21] The present analysis strongly supports its interpretation as a simple DOS effect. The disorder-induced broadening in the CPA is sufficient to make this peak effectively unobservable at intermediate compositions.

For the natural ^{13}C abundance of 1.1 at. %, the CPA yields a maximum disorder-induced broadening nearly two orders of magnitude smaller than that predicted by Bray and Anthony.[9] It follows that the disorder-enhanced umklapp-scattering mechanism proposed by those authors is unlikely to be responsible for the 50% increase in room-temperature thermal conductivity[3] as the ^{13}C concentration is reduced from 1.1 to 0.07 at. %. At frequencies below 1000 cm^{-1}, the present CPA results at all compositions are indistinguishable from those of weak-scattering perturbation theory.[22] Below 200 cm^{-1} the CPA relaxation time reduces to the usual ω^{-4} behavior characteristics of Rayleigh scattering[23] with a prefactor identical to that calculated by Klemens[24] for phonon-isotope scattering. *The present results are thus entirely consistent with the known effects of isotopic disorder on the thermal conductivity.*[23–25] In view of the limited data available,[3,26–28] it is difficult to predict the quantitative behavior of the thermal conductivity at different compositions with any degree of confidence. We limit ourselves here to demonstrating that a 50% increase (in thermal conductivity) upon elimination of the natural abundance of ^{13}C is indeed possible at room temperature given the expected reduction in phonon-isotope scattering, *provided that sufficient normal scattering also occurs.* (Note that such scattering contributes to the thermal resistance only indirectly by altering the phonon distribution.[23,25])

Section II of this paper describes the CPA formalism for diamond and the VCA reference spectra. Section III presents the first- and second-order Raman measurements and related CPA results. Additional CPA predictions and their implications for the composition dependence of the thermal conductivity are discussed in Sec. IV.

II. THEORY

A. Coherent-potential-approximation formalism

We assume that for any ^{13}C concentration x, the ^{12}C and ^{13}C isotopes are randomly distributed on an ideal diamond lattice. Since interatomic interactions are primarily chemical in nature, we further assume that the diamond force constants are independent of isotopic mass. This latter assumption is much more reliable here than it is in applications of the phonon CPA to chemically disordered alloys. The final simplification we make is to consider a purely harmonic model and neglect, except where indicated, the recently observed[29] fractional change in the lattice constant from ^{12}C to ^{13}C diamond of -1.5×10^{-4}. A more complete theory of isotopically mixed diamond would include both anharmonicity and disorder on an equal footing, but that is not attempted here.

Within the VCA each lattice site is assumed to be occupied by an identical atom of average mass $\overline{M}=12+x$ (in amu). Suppressing the x index, we denote the VCA phonon frequencies at wave vector $\mathbf{q}$ by $\omega_{\mathbf{q}j}$, where j is a branch index, and the VCA DOS (normalized to unity) as

$$g_{\mathrm{VCA}}(\omega)=(6N)^{-1}\sum_{\mathbf{q},j}\delta(\omega-\omega_{\mathbf{q}j}) , \tag{1}$$

where N is the number of unit cells in a normalization volume.

The phonon CPA is a multiple-scattering theory in which the true disordered system is replaced by a self-consistent effective medium.[5,6] This medium is characterized by a dimensionless self-energy $\tilde{\varepsilon}(\omega)$, which represents a complex "mass defect" relative to $\overline{M}$ at frequency ω. Self-consistency is imposed by the condition that the average scattering from a single site in the effective medium vanish. It is convenient to express this condition as[30]

$$\overline{M}\tilde{\varepsilon}(\omega)=\frac{x(1-x)(\Delta M)^2\omega^2F(\omega^2)}{1+\omega^2[(1-2x)\Delta M+\overline{M}\tilde{\varepsilon}(\omega)]F(\omega^2)} , \tag{2}$$

where ΔM is the 1-amu mass difference between ^{12}C and ^{13}C and $F(\omega^2)$ is the site Green's function:

$$\begin{aligned}F(\omega^2)&=(6N\overline{M})^{-1}\sum_{\mathbf{q},j}G_j(\mathbf{q},\omega^2)\\&=\frac{1}{\overline{M}}\int_0^\infty\frac{g_{\mathrm{VCA}}(\eta)d\eta}{\omega^2[1-\tilde{\varepsilon}(\omega)]-\eta^2} .\end{aligned} \tag{3}$$

The second line of Eq. (3) follows from the definition of the $\mathbf{q}$-space Green's function

$$G_j(\mathbf{q},\omega^2)=\frac{1}{\omega^2[1-\tilde{\varepsilon}(\omega)]-(\omega_{\mathbf{q}j})^2} , \tag{4}$$

whose negative imaginary part defines the CPA spectral function. With matrix element effects neglected, this spectral function is proportional to the Raman- and

neutron-scattering cross sections of interest below.[6] In the absence of disorder, $-\mathrm{Im}G_j(\mathbf{q},\omega^2)$ reduces to a δ function at $\omega_{\mathbf{q}j}$. To a good approximation,[10] the real and imaginary parts of $\tilde{\varepsilon}(\omega)$ shift the spectral peak to a frequency $\tilde{\omega}_{\mathbf{q}j}=\omega_{\mathbf{q}j}[1-\mathrm{Re}\tilde{\varepsilon}(\omega_{\mathbf{q}j})]^{-1/2}$ and broaden it to a full width at half maximum (FWHM) of $-\tilde{\omega}_{\mathbf{q}j}\mathrm{Im}\tilde{\varepsilon}(\tilde{\omega}_{\mathbf{q}j})$. The shift and broadening are related by the Kramers-Kronig relation[31]

$$\mathrm{Re}\tilde{\varepsilon}(\omega)=\frac{2}{\pi}\int_0^\infty \frac{\eta\,\mathrm{Im}[\tilde{\varepsilon}(\eta)]d\eta}{\eta^2-\omega^2} . \tag{5}$$

The normalized one-phonon CPA DOS is given by[5,10]

$$g(\omega)=-\frac{2}{\pi\omega}\int_0^\infty g_{\mathrm{VCA}}(\eta)d\eta\,\mathrm{Im}\left[\frac{\eta^2}{\omega^2[1-\tilde{\varepsilon}(\omega)]-\eta^2}\right] . \tag{6}$$

The CPA self-energy $\tilde{\varepsilon}(\omega)$ is formally independent of $\mathbf{q}$. An *implicit* $\mathbf{q}$ dependence does arise, however, through Eq. (4). The lack of an explicit $\mathbf{q}$ dependence is a consequence of the single-site nature of the CPA. In the limits of weak scattering ($\Delta M/\overline{M}\ll 1$) and/or dilute concentrations (both of which are approximately met for the natural abundance of ^{13}C), the CPA self-energy becomes exact and the $\mathbf{q}$ independence is rigorous.[7] In other regimes the CPA is a highly successful interpolation scheme and $\mathbf{q}$-dependent corrections should only appear at relatively high order in the scattering strength.[7]

It will be useful in Sec. IV to consider the weak-scattering limit explicitly. Equation (2) in this limit reduces to

$$\overline{M}\tilde{\varepsilon}(\omega)=x(1-x)(\Delta M)^2\omega^2F_{\mathrm{VCA}}(\omega^2) , \tag{7}$$

where $F_{\mathrm{VCA}}(\omega^2)$ is the VCA site Green's function, obtained by setting $\tilde{\varepsilon}(\omega)=0$ in Eq. (3). Using the fact that

$$-\mathrm{Im}F_{\mathrm{VCA}}(\omega^2)=\pi g_{\mathrm{VCA}}(\omega)/(2\overline{M}\omega) ,$$

we obtain the perturbative "golden-rule" expression for the FWHM broadening:

$$-\omega\,\mathrm{Im}\tilde{\varepsilon}(\omega)=\frac{\pi}{2}x(1-x)\left[\frac{\Delta M}{\overline{M}}\right]^2\omega^2g_{\mathrm{VCA}}(\omega) . \tag{8}$$

The full CPA equations (2) and (3) are easily solved numerically by an iterative process beginning with the VCA DOS. To speed up convergence, we take ω^2 to be complex, perform the calculations off the real axis, and analytically continue back to the real axis using the method of Hass, Velický, and Ehrenreich.[32] Explicit VCA dispersion relations are not required, and the VCA DOS needs to be specified only at one composition. The VCA scaling law $\omega_{\mathbf{q}j}\propto\overline{M}^{-1/2}$ implies that

$$g_{\mathrm{VCA}}(\omega)=R^{1/2}g_{12}(R^{1/2}\omega) , \tag{9}$$

where $R=(1+x/12)$ and $g_{12}(\omega)$ is the DOS for pure ^{12}C diamond. We make use of this result in Eq. (3) and evaluate the site Green's function at any composition as

$$F(\omega^2)=\frac{R}{\overline{M}}\int_0^\infty \frac{g_{12}(\xi)d\xi}{R\omega^2[1-\tilde{\varepsilon}(\omega)]-\xi^2} . \tag{10}$$

B. Virtual-crystal dispersion curves and densities of states

The above formalism was implemented in I using the TPZ valence-force model.[11] This model provides an excellent fit to experimental phonon frequencies for natural diamond, which have been determined by inelastic neutron scattering.[15] The TPZ parametrization consists of six valence-force parameters, including a fifth-neighbor, coplanar angle-angle interaction first introduced by McMurry *et al.*[33] We have found it convenient to transform these parameters to a Born–von Kármán description using the results of Tubino and Piseri.[34] The dynamical matrix is then as specified by Herman.[35] The resulting dispersion curves for a VCA description of natural diamond are shown in Fig. 1. The Raman mode corresponds to the zone-center optic phonon, whose frequency we denote as $\omega_{\mathrm{LTO}}(\Gamma)$. The upper portion of the figure shows an enlargement of the dispersion curves in the vicinity of this mode. Note especially the slight increase in the LO branch along the Γ-X direction which produces a maximum phonon frequency 2.2 cm^{-1} higher than $\omega_{\mathrm{LTO}}(\Gamma)$. This characteristic feature of the TPZ model[12] is difficult to verify experimentally because of the poor resolution of neutron scattering at high frequencies. In the other principal directions, the TPZ model predicts a monotonic decrease in the frequencies of the LO and TO branches away from Γ. All of the curves in Fig. 1, including the fine structure near $\omega_{\mathrm{LTO}}(\Gamma)$, are in excellent agreement with previously published results.[11,12]

Figure 2 shows the VCA DOS calculated for the TPZ model using the tetrahedron method[36] and a mesh of over 5000 $\mathbf{q}$ points in the irreducible Brillouin zone. The inset again shows an enlargement of the region near the Raman mode. Figure 2 is in reasonable agreement with the

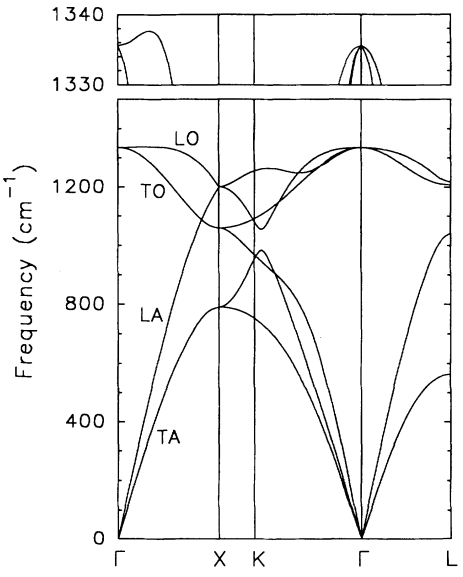

FIG. 1. Virtual-crystal dispersion curves for naturally abundant diamond (1.1 at. % ^{13}C) calculated from TPZ parameters. Branches along Γ-X identified as to longitudinal (L) vs transverse (T), acoustic (A) vs optic (O) character. Top shows enlargement in vicinity of Raman mode.

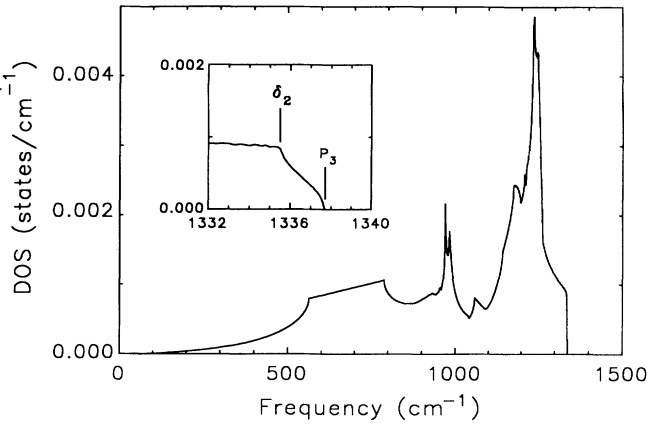

FIG. 2. Normalized virtual-crystal density of states [cf. Eq. (1)] corresponding to Fig. 1. The inset shows the behavior near the Raman mode (a δ_2 fluted saddle point) and the P_3 maximum on an expanded scale.

original, low-resolution histogram published by TPZ.[11] The present results contradict, however, the "higher-resolution" calculations of Tubino and Birman.[12] These authors found a peak in the DOS at $\omega_{\mathrm{LTO}}(\Gamma)$ which they attributed to the unusual dispersion relations in Fig. 1, which make Γ a δ_2 fluted saddle point.[37] We find no evidence for such a peak and see only the type of DOS behavior expected at a δ_2 singularity[38] and at the P_3 maximum along Γ-X. To test our integration routine, we have performed additional brute-force root-sampling calculations using a much larger number of **q** points (over 10^5); the results are indistinguishable from those in Fig. 2. We conclude that the figure is correct and that the TPZ model *does not* give a peak in the DOS near $\omega_{\mathrm{LTO}}(\Gamma)$.

The importance of this conclusion will be seen more clearly in Sec. III. Note that the work of Tubino and Birman[12] was an attempt to explain the origin of the sharp peak near the top of the second-order Raman spectrum of diamond.[13] This peak appears at a few cm^{-1} above twice $\omega_{\mathrm{LTO}}(\Gamma)$ and has an intrinsic width[14] of approximately 4.2 cm^{-1}. The origin of this peak has generated much controversy over the years. Recent calculations of anharmonic effects in diamond[20,21] do not support the model of a two-phonon bound state,[16] but it is still unclear whether this peak is a consequence of matrix-element effects[18,19] or whether it is simply a feature of the overtone DOS (Refs. 12 and 17) (i.e., the one-phonon DOS with the frequency scale doubled). The (spurious?) results of Tubino and Birman[12] led those authors to champion the last of these possibilities. In fact, we believe that this is the correct explanation, although Fig. 2 shows that the TPZ model itself is not sufficient to produce an overtone peak.

To see how such a peak might arise, we consider in Fig. 3 four sets of dispersion curves for pure ^{12}C diamond in the vicinity of the Raman mode. These curves were calculated using the tensor-force constants listed in Table I (in Herman's notation[35]). The set labeled "TPZ" corresponds to the original TPZ parameters[11] multiplied by 0.995 to improve the agreement with the experimental Raman frequencies in Sec. III. The three modified sets, labeled $M1$, $M2$, and $M3$, are obtained by adjusting a single force constant in each case. The motivation for these particular adjustments is apparent from Fig. 3. $M1$ makes $\omega_{\mathrm{LTO}}(\Gamma)$ the maximum phonon frequency, which is the case in Si and Ge (Refs. 10 and 15) and which, prior to the work of Tubino and Birman,[12] was believed to be the case in diamond as well. By contrast, the LO branch increases away from Γ along one, two, and three principal directions in the "TPZ," $M2$, and $M3$ parametrizations, respectively. The corresponding DOS in each case is shown in Fig. 4. The "TPZ" curve is similar to the in-

TABLE I. Force constants (in mdyn/Å), in notation of Ref. 35, for rescaled model ("TPZ") of Ref. 11 and modified models $M1$, $M2$, and $M3$.

Force constant	"TPZ"	Modifications
α	1.4951	
β	0.3761	
μ	0.2408	($\rightarrow$0.18 in $M1$)
λ	−0.2587	
ν	0.2313	($\rightarrow$0.39 in $M2$)
δ	0.1784	
μ'''	0.0120	
λ'''	0.0483	
ν'''	0.0120	($\rightarrow$0.25 in $M3$)
δ'''	−0.0242	

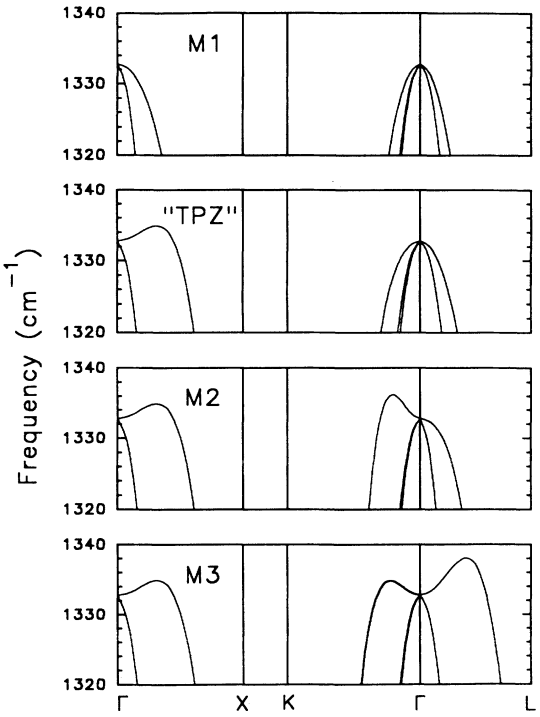

FIG. 3. Highest-frequency dispersion curves for pure ^{12}C diamond calculated from the "TPZ" and modified ($M1$,$M2$,$M3$) parameter sets in Table I. The Raman mode is the same in each case.

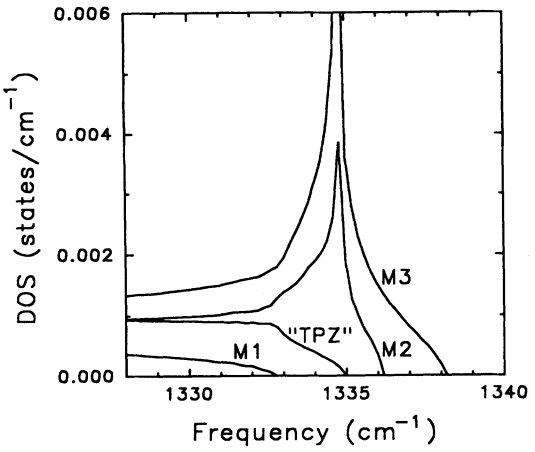

FIG. 4. Normalized densities of states corresponding to Fig. 3.

set in Fig. 2, and the $M1$ curve goes to zero at $\omega_{\mathrm{LTO}}(\Gamma)$. Both the $M2$ and $M3$ curves, however, exhibit peaks a few cm^{-1} above $\omega_{\mathrm{LTO}}(\Gamma)$. The positions of these peaks correspond to subsidiary maxima along principal directions in Fig. 3 that are not the absolute maxima of the spectra.

It thus appears that the existence of a peak near the top of the one-phonon DOS in diamond requires that the LO branch increase along at least *two* principal directions, not just one. This possibility was first suggested by Uchinokura, Sekine, and Matsuura[17] and is consistent with the recent tight-binding calculations of Wang Chan, and Ho.[21] An attractive consequence of this proposal is that it accounts naturally for the few cm^{-1} shift of the observed second-order Raman peak[13,14] above twice $\omega_{\mathrm{LTO}}(\Gamma)$; this shift was not accounted for in the results of Tubino and Birman.[12] Further evidence that the true dispersion curves for diamond are closer to those of models $M2$ or $M3$ than $M1$ or "TPZ" will be presented in Sec. III of this paper. We have already mentioned that it would be difficult to verify this behavior directly by neutron scattering because of the fine resolution required. First-principles calculations for diamond[20] do indicate a slight increase in the LO-phonon frequency along Γ-X, but similar calculations for other directions have yet to be performed.

Although models $M2$ and $M3$ are useful for illustrative purposes, neither of these models should be viewed as an "improved" parametrization for diamond. The qualitative changes near $\omega_{\mathrm{LTO}}(\Gamma)$ in these models are accompanied by much more disruptive changes at lower frequencies where the unmodified "TPZ" model is known to be accurate. In principle, a new overall fit might allow one to maintain the "TPZ" dispersion curves at low frequencies while simultaneously "correcting" the behavior near $\omega_{\mathrm{LTO}}(\Gamma)$. Since the CPA does not require explicit dispersion curves, we have not attempted such a fit and instead simply modify the VCA DOS directly. We do this by adding to the "TPZ" DOS the artificial correction shown in Fig. 5(a). The motivation for this particular form of correction will become more apparent from the discussion of the second-order Raman spectrum in Sec. III B. The correction vanishes below 1200 cm^{-1}, as does its integral over frequency (which is required to maintain normalization). The high-frequency portion of the resulting ^{12}C reference DOS [g_{12} in Eq. (10)] is shown in Fig. 5(b); we will refer to calculations based on this reference as the adjusted "TPZ" model.

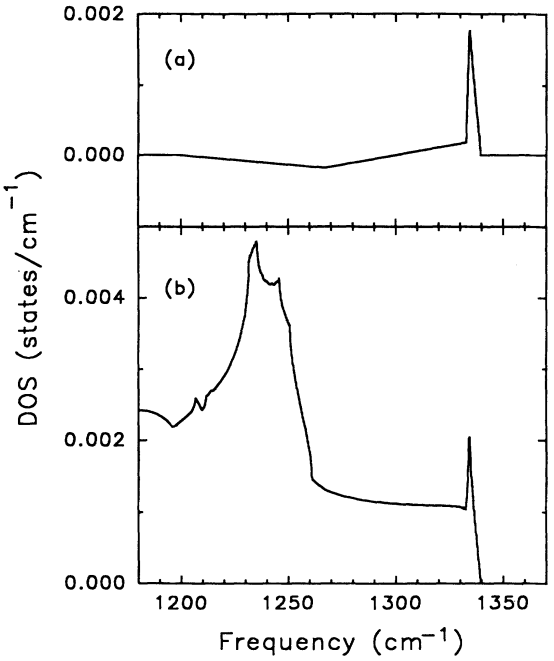

FIG. 5. (a) Correction added to "TPZ" density of states for pure ^{12}C diamond to introduce a peak above the Raman mode. (b) Resulting reference density of states for the adjusted "TPZ" model.

III. COMPARISON TO RAMAN DATA

A. First-order spectra

Natural diamond exhibits a single first-order Raman peak at $\omega_{\mathrm{LTO}}(\Gamma)=1332.5$ cm^{-1}. We know of only two reports prior to our own work of Raman measurements on single-crystal diamonds with other isotopic compositions. Collins *et al.*[39] cite an unpublished measurement by Sato of a Raman frequency of 1282 cm^{-1} for a 99-at. % ^{13}C diamond. Chrenko[40] has presented more extensive data across the entire composition range. Our own measurements, which were discussed briefly in I, agree well with both of these studies. Additional Raman data on isotopically mixed *polycrystalline* diamond films[41] will not be considered here because of the numerous extrinsic factors[42] (e.g., stress, impurities) that can obscure the intrinsic composition dependence in such films.

The synthetic diamonds we examined were grown at GE by a technique that has been described elsewhere.[1,2] Raman spectra were measured on five crystals with ^{13}C concentrations[43] x of 0.0007, 0.011, 0.344, 0.657, and

0.9899. These same crystals had been characterized previously by x-ray diffraction and found to be of exceptional crystal quality;[29] their Bragg-peak widths are comparable to those of good semiconductor crystals. The Raman measurements were made at room temperature using the 5145-Å excitation line of an argon-ion laser, a 1-m $f/8$ spectrometer, and a photomultiplier detector. The samples were mounted in a near-normal backscattering geometry with the axis of the objective lens normal to a $\langle 100 \rangle$ crystal face. The system was calibrated against a Hg vapor line and found to have an instrumental linewidth (FWHM) of 1.8 cm^{-1}. Only unpolarized spectra were recorded.

The measured frequencies and widths of the first-order Raman lines are plotted in Fig. 6 along with the data of Chrenko.[40] Both sets of data indicate that the Raman frequency varies nonlinearly with ^{13}C concentration. The deviation from linearity is approximately 5 cm^{-1} near the middle of the composition range. This is much larger than the experimental uncertainties [about the size of the data points in Fig. 6(a)] and should certainly be considered if the Raman frequency is to be used as a measure of isotopic composition. The linear Raman variation assumed in Ref. 41, for example, suggests that the x values determined in that work may be in error by as much as 0.1.

Also shown in Fig. 6(a) are the VCA prediction (dotted curve) and CPA results for both the pure (dashed curve) and adjusted (solid curve) "TPZ" models. All of the calculated frequencies include a small *ad hoc* correction[44] to account for the observed lattice contraction from ^{12}C to ^{13}C diamond.[29] The "bowing" of the Raman frequency is well reproduced by both CPA curves, but not by the VCA. (The VCA curve does in fact bow slightly, but in the wrong direction.) We conclude that the bowing is a direct consequence of the scattering of phonons due to isotopic disorder. Since the Raman mode lies near the top of the spectrum, it is repelled upward by disorder-induced mixing with lower-lying modes. A similar nonlinear concentration dependence is observed in many other properties of disordered alloys (e.g., band gaps in semiconductors[45]).

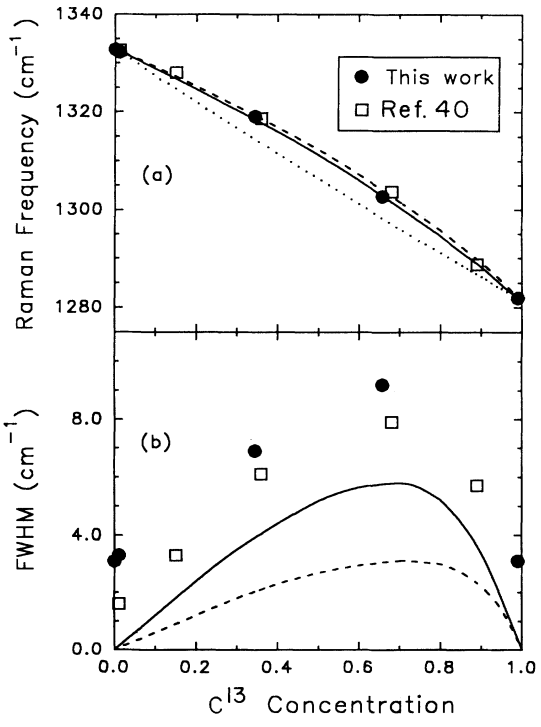

FIG. 6. Isotopic composition dependence of the (a) diamond Raman frequency and (b) linewidth (FWHM). CPA results for pure and adjusted "TPZ" models and VCA results in (a) shown as dashed, solid, and dotted lines, respectively. Experimental data as indicated. Chrenko's data are taken from Ref. 40.

The measured Raman linewidths [Fig. 6(b)] are larger near the center of the composition range than near the end points. The variation is not symmetric in x and $1-x$, and the maximum width occurs at approximately 70 at. % ^{13}C. The CPA curves represent intrinsic contributions to the Raman linewidth due to the disorder-induced broadening of the zone-center optic mode. The observed widths contain additional contributions due to instrumental resolution (1.8 cm^{-1} for our data) and anharmonic decay.[10,46] The anharmonic broadening of the Raman line has been calculated for diamond[46] to be on the order of 1 cm^{-1} at 300 K. Contributions other than disorder thus account well for the observed widths near $x=0$ and 1. Assuming that such contributions are reasonably constant across the entire composition range, we see that both CPA calculations account very well for the qualitative trend in the data, including the peak near $x=0.7$. The pure "TPZ" model underestimates the magnitude of the variation, however, by about a factor of 2. The adjusted "TPZ" model of Fig. 5 overcomes this deficiency and yields quantitative as well as qualitative agreement.

The larger broadening in the adjusted "TPZ" model results from the larger DOS available for scattering at the shifted position of the Raman mode. The calculated shifts in Fig. 6(a) are much less sensitive to the existence

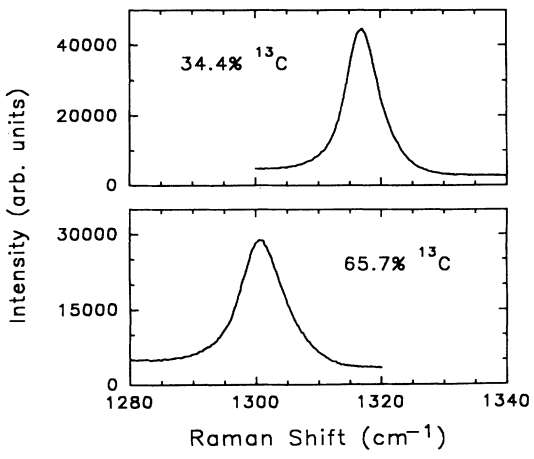

FIG. 7. First-order Raman spectra for a 34.4 at. % ^{13}C (top) and a 65.7 at. % ^{13}C (bottom) synthetic diamond.

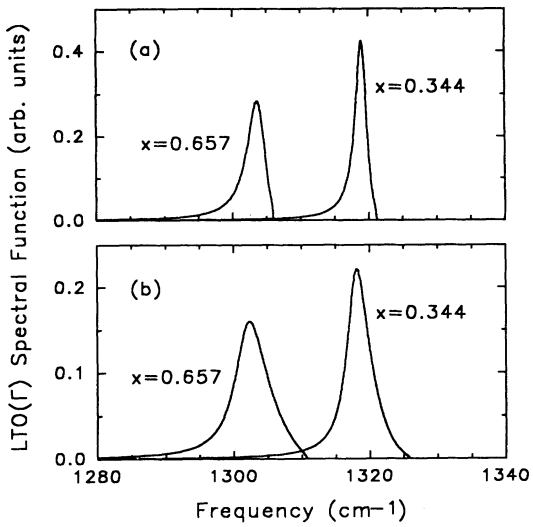

FIG. 8. CPA spectral functions for the LTO (Γ) modes calculated in the (a) pure and (b) adjusted "TPZ" models for $x=0.344$ and 0.657.

of a peak in the VCA DOS since the real part of $\bar{\varepsilon}(\omega)$ is determined by scattering over an extended frequency range [cf. Eq. (5)]. Figure 6 thus provides strong support for the assumption that the true VCA DOS for diamond should contain a peak above $\omega_{\mathrm{LTO}}(\Gamma)$. Even more apparent is the fact that the observed broadening of the Raman line is completely inconsistent with the Raman mode being the highest-frequency phonon in diamond (e.g., as in model $M1$ in Fig. 3). The calculated CPA broadening in that case would be $\ll 1$ cm^{-1} across the entire composition range since the shifted Raman mode would lie in a region where the VCA DOS is zero. This is the situation that occurs in Ge; the width of the Ge Raman line is unaffected by isotopic enrichment[10] (from the natural abundances of 22 at. % ^{70}Ge, 28 at. % ^{72}Ge, 8 at. % ^{73}Ge, 35 at. % ^{74}Ge, and 7 at. % ^{76}Ge to nearly pure ^{70}Ge), in strong contrast to the behavior in Fig. 6(b).

Still further evidence for the existence of a peak near the top of the diamond DOS is provided by the *shapes* of the Raman lines. Figure 7 shows the measured spectra for the 34.4-at. % and 65.7-at. % ^{13}C crystals. The observed lines are almost completely symmetric and have a nearly Lorentzian shape. Figure 8 shows the corresponding CPA zone-center spectral functions for the (a) pure and (b) adjusted "TPZ" models. The pure "TPZ" model gives a highly asymmetric line shape because of the rapid falloff of the DOS on the high-frequency side of the Raman mode. The more symmetric line shapes for the adjusted "TPZ" model are much closer to those observed.

The above considerations may explain, in part, why the widely used spatial correlation model[47] has been unsuccessful in describing the shift and broadening of the first-order Raman line in microcrystalline diamond.[48] This model assumes that the dispersion curves in the vicinity of the Raman mode are well known, which we have seen is not at all the case in diamond.

B. Second-order spectra

Second-order Raman spectra for the same five synthetic diamonds considered above are shown in Fig. 9. The second-order spectra were measured with a slightly lower resolution (~ 4 cm^{-1}) than the first-order spectra because of the much lower count rate. The present results for 1.1 at. % ^{13}C agree well with previous measurements for natural diamond.[13,14] The spectra for 0.07 and 99 at. % ^{13}C also look similar, if one ignores the shifts that occur as a result of differences in $\bar{M}$. More significant differences are observed for the more heavily mixed crystals; the 34.4 and 65.7 at. % ^{13}C results are noticeably broader and do not appear to exhibit the sharp peak near the high-frequency cutoff. It is this peak at the top of the second-order spectrum (2667 cm^{-1} for 1.1 at. % ^{13}C) that we already mentioned has been the subject of intense controversy. Chrenko[40] also examined the second-order spectra of his samples and claims that he was able to see this peak at all compositions except 68 at. % ^{13}C. His measurements may have been of somewhat higher resolution than ours, but it is clear that even in his 89 at. % ^{13}C spectrum (which is the only raw data presented), some broadening of this peak has occurred.

A full calculation of the second-order Raman spectrum is beyond the scope of this work. Such a calculation requires the consideration of all possible two-phonon excitations in which the net wave vector is zero $[\omega_i(\mathbf{q})+\omega_j(-\mathbf{q})]$. The frequencies of the two phonons

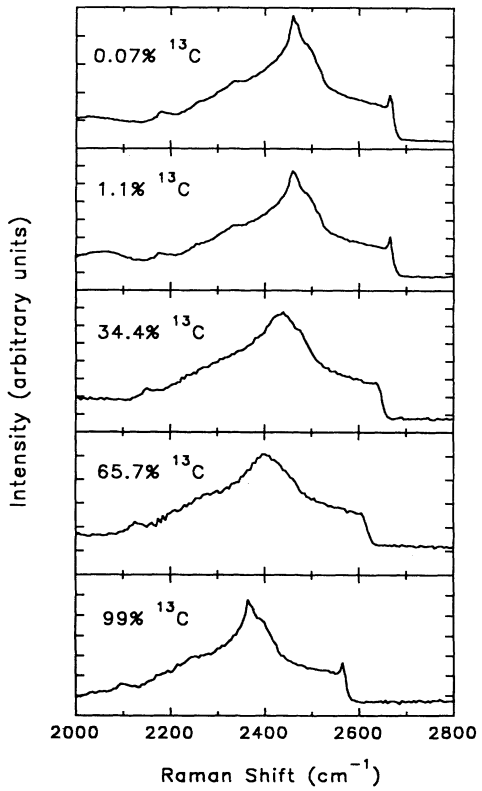

FIG. 9. Second-order Raman spectra for synthetic diamond with the indicated compositions.

may be the same (an overtone, $i=j$) or different (a combination, $i\neq j$). Relative intensities may be strongly affected by selection rules and other matrix-element effects.[18,19] Solin and Ramdas[13] extensively analyzed the second-order Raman spectrum of diamond and assigned much of the fine structure to particular overtones and combinations of phonons at high-symmetry points. They left open, however, the interpretation of the 2667-cm^{-1} peak because this did not arise naturally from any of the dispersion curves available at that time.

For our purposes it suffices to consider the overtone DOS alone as a crude approximation to the second-order Raman spectrum.[49] Figure 10 shows the calculated CPA DOS's for the adjusted "TPZ" model for the same compositions as in Fig. 9; the solid curves are Lorentz broadened by 1.5 cm^{-1} to simulate the experimental resolution. Comparison of the resulting overtone DOS (obtained by doubling the frequency scale in Fig. 10) for $x=0.011$ to the corresponding experimental spectrum in Fig. 9 shows reasonable agreement both for the most prominent peak near 2460 cm^{-1} and for the 2667-cm^{-1} peak. This comparison helps to justify the particular form of DOS peak added in Fig. 5. CPA results for other compositions reproduce very well the observed trends in the second-order spectra, including both the broadening of the main peak and the disappearance of the high-frequency peak for $x=0.344$ and 0.657. This latter effect is a consequence of the increased "effective" scattering strength in the vicinity of a sharp structure.[7] Together with the evidence presented in Sec. III A, the present results make a strong case for both the reasonableness of the CPA description of disorder effects and for the interpretation of the sharp peak at the top of the second-order spectrum as a simple DOS effect.

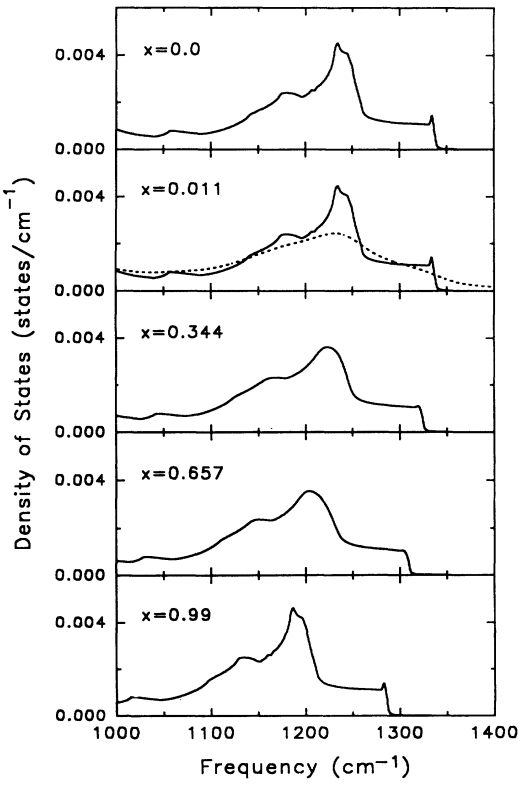

FIG. 10. CPA densities of states (based on the adjusted "TPZ" model) for the indicated concentrations of ^{13}C. Solid curves are Lorentz broadened by 1.5 cm^{-1} to provide more meaningful comparison to Fig. 9. Dashed curve for $x=0.011$ is broadened by 50 cm^{-1}.

IV. ADDITIONAL CPA RESULTS AND THERMAL CONDUCTIVITY

A more complete set of CPA predictions for isotopically mixed diamond is given in Fig. 11. Recall that the calculated shifts and broadenings of phonon modes are related by Eq. (5). The qualitative similarities between the CPA results at different compositions are a consequence of the small $\Delta M/\overline{M}$ values in diamond. In the weak-scattering limit [Eq. (8)], the frequency dependence of the broadening closely follows that of the VCA DOS. Below 1000 cm^{-1} the full CPA results for diamond are indistinguishable from those calculated in this limit across the entire composition range.

At higher frequencies significant deviations from weak-scattering behavior do occur. The dashed curves in Fig. 11 show the calculated weak-scattering broadenings for $x=0.25$ and 0.75. Relative to these curves, the full CPA predicts a larger (smaller) broadening at the very top of the spectrum for $x=0.75$ ($x=0.25$) and a smaller (larger) broadening at slightly lower frequencies (≈ 1150 cm^{-1}). These differences reflect the fact that the magnitude of the scattering in a more strongly scattering alloy is enhanced in those portions of the spectrum where the

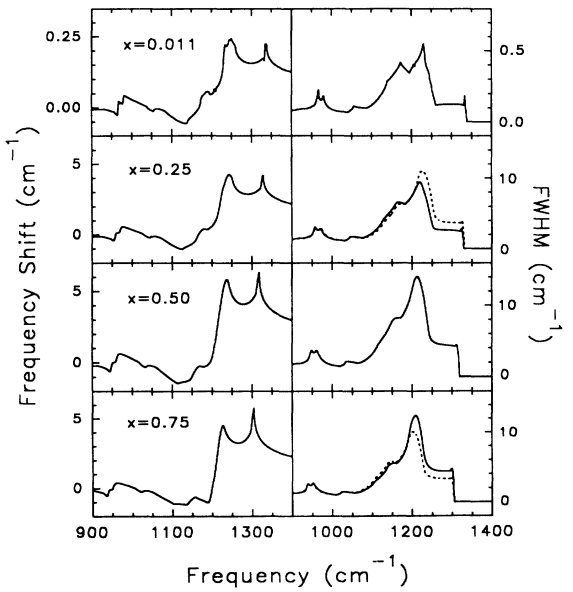

FIG. 11. CPA frequency shifts (left) and FWHM broadenings (right) calculated for the indicated concentrations of ^{13}C in the adjusted "TPZ" model. Dashed curves on right for $x=0.25$ and 0.75 obtained from the weak-scattering expression [Eq. (8)].

minority-species contribution is largest.[7] For $x<0.5$ the enhancement occurs below the main DOS peak because the minority ^{13}C species is heavier than the majority species. Conversely, for $x>0.5$ the enhancement occurs above this peak because the minority ^{12}C species is lighter than the majority species. It is precisely this enhancement of minority scattering that is responsible for the asymmetric composition dependence of the Raman linewidths in Fig. 6(b). Since the Raman mode lies near the top of the spectrum, it is more sensitive to isotopic disorder for $x>0.5$. Weak-scattering perturbation theory, by contrast, incorrectly predicts a nearly symmetric composition dependence.

The relatively small magnitude of the disorder effects in Fig. 11 is in sharp contrast to the Bray and Anthony[9] estimate of a 50-cm^{-1} broadening at large wave vectors for all $0.011 \leq x \leq 0.989$. Such a large broadening would certainly have been seen in the second-order Raman spectra of Fig. 9; to emphasize this point, the dashed curve in Fig. 10 for $x=0.011$ has been broadened by this amount.[50] The Bray-Anthony estimate is based on the difference between phonon frequencies in the pure ^{12}C and pure ^{13}C limits. It is well known that such Lifshitz-like limits[51] provide only a weak upper bound on the actual broadening that occurs in a disordered alloy.[7] The present CPA results yield a maximum broadening of less than 15 cm^{-1} for $x=0.5$ and of less than 0.6 cm^{-1} for $x=0.011$. (Note the change in scale for $x=0.011$ in Fig. 11.) The CPA also gives a much more realistic composition dependence [dominated by the $x(1-x)$ factor in Eq. (2)] than that assumed by Bray and Anthony.

In principle, the present CPA results for any phonon mode may be directly tested by inelastic neutron scattering. Since the predicted deviations from VCA behavior are small, however, it is unclear whether this technique has sufficient resolution to observe such effects. As examples of what to expect in such experiments, we plot in Figs. 12 and 13 the relevant CPA spectral functions for two different zone-boundary states at three different compositions. The transverse-acoustic mode at L in Fig. 12 remains very sharp (FWHM <1 cm^{-1}) at all compositions. The doubly degenerate longitudinal mode at X in Fig. 13 lies in a much stronger-scattering region, but still has a width of less than 8 cm^{-1} for $x=0.5$. The effects of anharmonic broadening on these modes may again be estimated from Ref. 46.

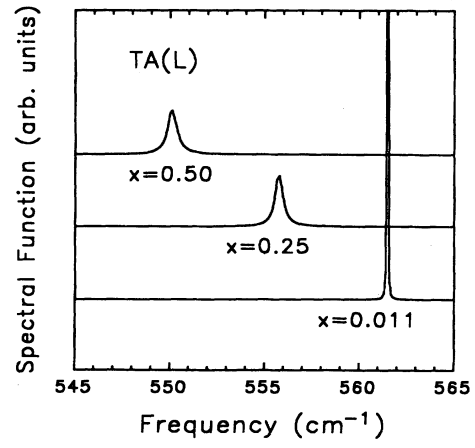

FIG. 12. CPA spectral functions for the TA(L) mode at the indicated concentrations of ^{13}C.

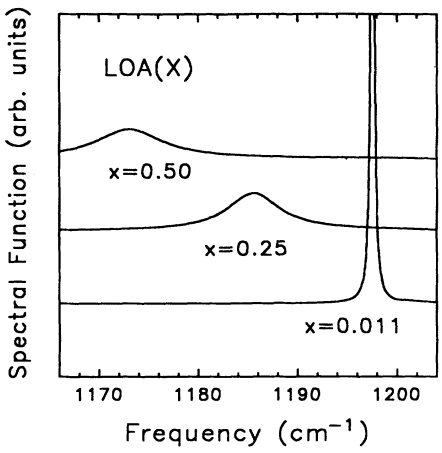

FIG. 13. Same as Fig. 12, but for the LOA(X) mode.

We now consider whether the CPA can account for the observed strong dependence of the thermal conductivity of diamond on isotopic composition.[3] An important caveat to keep in mind in this discussion is that it is still unclear experimentally whether the observed enhancement in room-temperature thermal conductivity for $x<0.011$ is purely an intrinsic effect or whether extrinsic factors also play a role.[52] The x-ray measurements of Holloway *et al.*[29] rule out the possibility of gross structural differences between $x=0.011$ and lower-x GE synthetic diamonds, but more subtle differences (e.g., in impurity concentrations) may be present.

The small disorder effects predicted by the CPA for $x=0.011$ have a negligible effect on both the specific heat and velocities of low-frequency phonons. The insensitivity of the specific heat to small concentrations of ^{13}C has been confirmed experimentally by Morelli *et al.*[26] It follows from these considerations that the strong dependence of the thermal conductivity on isotopic composition must be due to changes in phonon-scattering rates.

The possible importance of phonon scattering by isotopes was first suggested by Pomeranchuk.[53] Using perturbation theory, Klemens[24] showed that the scattering rate due to a concentration x of point defects differing only in mass is

$$\tau^{-1}(\omega)=\frac{x(1-x)V_0}{4\pi v^3}\left[\frac{\Delta M}{\overline{M}}\right]^2\omega^4 , \tag{11}$$

where v is the average phonon velocity (assuming no dispersion) and V_0 is the volume per atom (5.7×10^{-24} cm^3 here). This expression has the usual ω^4 dependence of classical Rayleigh scattering.[23] For $x=0.011$, the "TPZ" model considered in this paper yields $v=1.3\times10^6$ cm/sec; the resulting prefactor in Eq. (11) has the numerical value $A=0.019$ $sec^{-1}cm^4$. The frequency dependence of the scattering rate in this case is

plotted as a dashed curve in Fig. 14. For comparison, the solid curve shows the CPA scattering rate for $x=0.011$, determined from the FWHM broadening. The good agreement below 200 cm^{-1} implies that Eq. (11) is reasonable up to room temperature. The stronger CPA scattering rate at higher frequencies is due to the dispersion of the TA branches[22] in Fig. 3. Throughout the entire range of Fig. 14, the CPA rate is well described by the weak-scattering expression [Eq. (8)]. Below 200 cm^{-1}, $g_{VCA}(\omega)$ may be replaced by the Debye DOS (Ref. 8) $V_0\omega^2/(2\pi^2v^3)$, which makes Eq. (8) formally equivalent to Eq. (11).

The CPA is thus entirely consistent with the standard theory of phonon-isotope scattering.[23–25] Recently, Bray and Anthony[9] suggested that, in addition to this direct effect, isotopic disorder might also have an indirect effect on other scattering processes that affect the thermal conductivity. In particular, they argued that the broadening of the phonon-dispersion curves near the zone boundaries might significantly enhance umklapp scattering. The magnitude of this enhancement depends exponentially on the broadening.[9] For the 50-cm^{-1} broadening for $x=0.011$ assumed in Ref. 9, this mechanism predicts a 63% reduction in the room-temperature thermal resistance due to umklapp scattering upon elimination of the ^{13}C impurities. The much smaller CPA broadening, however, predicts less than a 1% reduction. We conclude that the indirect effects of isotopic disorder are negligible in the CPA and that the origin of the observed thermal conductivity enhancement must lie in Eq. (11).

In practice, a quantitative test of this hypothesis is highly nontrivial. The problem lies in the uncertainties associated with other scattering mechanisms: in particular, with phonon-phonon scattering, which is classified as either unklapp (U) or normal (N), depending on whether a reciprocal lattice vector is or is not involved.[23,25] In principle, the absolute scattering rates for these processes can be calculated from a knowledge of the full anharmonic potential of diamond. While some progress has been made in calculating this potential,[20,21] the implications of such work for the scattering rates of interest here have yet to be addressed. Most previous "theories" of thermal conductivity[23,54] have been based on phenomenological relaxation times whose predictive power is highly questionable. Complicating matters further is the fact that N and U processes do not contribute in the same way to the thermal conductivity. Only U processes increase the thermal resistance directly; N processes may still be important, however, because of their ability to scatter low-frequency phonons to higher frequencies where other resistive-scattering processes may be more effective.[23,25,54]

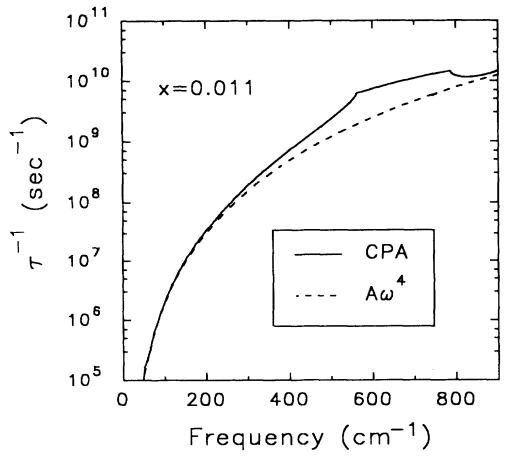

FIG. 14. Inverse relaxation time for naturally abundant diamond calculated in the CPA (solid curve) and from Eq. (11) (dashed curve); $A=0.019\ sec^{-1}\,cm^4$.

The most successful method for including N processes as well as resistive scattering is that of Callaway.[54] For a Debye model, which is sufficient here, the thermal conductivity in this approach reduces to a sum of two terms:

$$\kappa=\kappa_1+\kappa_2\ , \tag{12}$$

where

$$\kappa_1=GT^3\int_0^{\Theta/T}\tau_c J_4(\zeta)d\zeta\ , \tag{13}$$

$$\kappa_2=\frac{GT^3\left[\int_0^{\Theta/T}(\tau_c/\tau_N)J_4(\zeta)d\zeta\right]^2}{\int_0^{\Theta/T}(\tau_c/\tau_N\tau_R)J_4(\zeta)d\zeta}\ , \tag{14}$$

Θ is the Debye temperature, $\zeta=\hbar\omega/(kT)$, $G=k^4/(2\pi^2v\hbar^3)$, and $J_4=\zeta^4e^\zeta(e^\zeta-1)^{-2}$; τ_N and τ_R are the relaxation times for N processes and resistive scattering, respectively, and $\tau_C^{-1}=\tau_N^{-1}+\tau_R^{-1}$ is the total scattering rate.

Most previous work on diamond has neglected normal scattering completely[55–58] ($\tau_N\to\infty$), in which case $\kappa_2\to 0$. This approximation is clearly inadequate as the ^{13}C concentration is reduced since at some point the normal-scattering rate must exceed the isotope-scattering rate given by Eq. (11).

The other limiting case, in which normal scattering dominates, is more interesting to consider. In this case, $\tau_C\to\tau_N$, $\tau_N\ll\tau_R$, and $\kappa\to\kappa_2$. The thermal resistance $W=1/\kappa$ is then additive, and the contribution of any particular resistive process j is given by[59]

$$W_j=\frac{\int_0^{\Theta/T}\tau_j^{-1}J_4(\zeta)d\zeta}{GT^3\left[\int_0^{\Theta/T}J_4(\zeta)d\zeta\right]^2}\ . \tag{15}$$

Substitution of Eq. (11) in Eq. (15) gives exactly the same result as that obtained by Ziman using a variational method.[60] For $x=0.011$ and $\Theta=2165$ K (consistent with our choice of $v=1.3\times10^6$ cm/sec), the predicted value of $\kappa_j=1/W_j$ for isotope scattering at 300 K is 37 $W\,cm^{-1}\,K^{-1}$. Since the experimental value of κ for natural diamond[3,55] at 300 K is roughly 22 $W\,cm^{-1}\,K^{-1}$, this implies that the room-temperature thermal conductivity in the absence of isotope scattering is 54 $W\,cm^{-1}\,K^{-1}$ (a 150% enhancement). Equation (15), of course, represents only an upper bound on the thermal resistance since any reduction in normal scattering would tend to make

resistive-scattering processes less effective.[25] Nevertheless, this exercise shows that, for sufficiently strong normal scattering, the thermal resistance due to isotopes can easily account for a significant fraction of the total room-temperature thermal resistance in diamond.[61]

Further progress using the Callaway theory requires the consideration of explicit forms of the relaxation times due to other scattering mechanisms.[59] For illustrative purposes we choose here a normal-scattering rate $\tau_N^{-1}=0.011\zeta T^5$ and a resistive-scattering rate

$$\tau_R^{-1}=10^7+0.41x(1-x)\zeta^4T^4+0.9\zeta^2T^4e^{-500/T}$$

(both in $\sec^{-1}$). The three terms in τ_R^{-1} describe boundary scattering[62] (for a crystal roughly 1 mm on a side), isotope scattering [from Eq. (11)], and umklapp scattering,[59] respectively. The particular forms chosen here for N and U processes have no rigorous justification, but they do provide a reasonable description of the thermal conductivity of naturally abundant diamond over a broad temperature range.[55] The solid curve in Fig. 15(a) was obtained by substituting these expressions into Eqs. (12)–(14) for $x=0.011$. For comparison, the dashed curve shows the corresponding results obtained with normal scattering neglected. The purpose of this comparison is to emphasize that normal scattering can have a profound effect on the results everywhere except at the very lowest temperatures where boundary scattering dominates. Since it is conceivable that equally good fits to a given data set may be obtained with different functional forms and even different scattering mechanisms, the predictive power of this phenomenological approach is clearly limited.

Nevertheless, it is interesting to consider the results in Fig. 15(b) for different isotopic compositions based on the above scattering rates. Consistent with the available data,[3] we see a rapid falloff in the thermal conductivity at 300 K for very small concentrations of ^{13}C and a less rapid reduction at higher x. These calculations are intended simply as a plausibility argument that the observed composition dependence of the room-temperature thermal conductivity in diamond can, in fact, be explained using existing theory.[63] Data on the composition dependence at lower temperatures, near the thermal-conductivity peak, will be much more revealing. As seen in Fig. 15(b), the maximum thermal conductivity in pure ^{12}C diamond at liquid-nitrogen temperatures may well exceed 1000 W $cm^{-1}K^{-1}$, as suggested by others.[64]

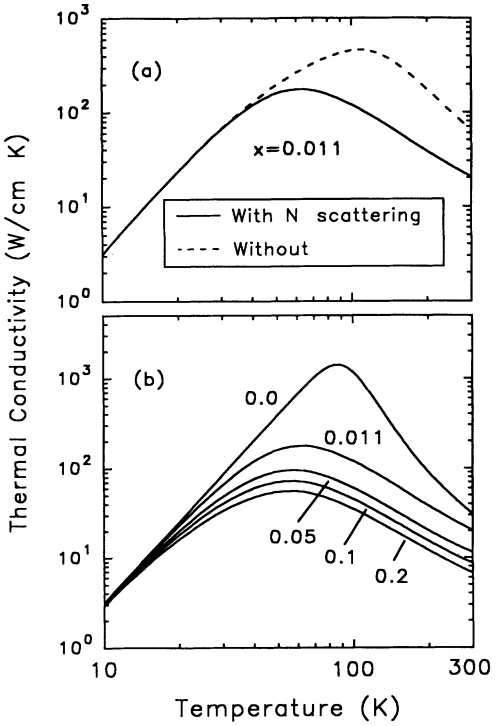

FIG. 15. Thermal conductivities calculated from Callaway's theory [Eqs. (12)–(14)] with relaxation rates given in text. (a) shows the importance of normal (N) scattering processes in this model for naturally abundant diamond. (b) gives results including N scattering for the ^{13}C concentrations indicated.

ACKNOWLEDGMENTS

We wish to thank Jim Fleischer, Dick Chrenko, Eoin O'Tighearnaigh, and Suresh Vagarili for their help in obtaining the diamonds used in this work and Craig Davis, Henry Ehrenreich, Jack Fischer, Joseph Heremans, Harry Holloway, David Onn, and Mike Thorpe for helpful discussions.

[1]W. F. Banholzer, T. R. Anthony, and R. Gilmore, in *Proceedings of the Second International Conference on New Diamond Science and Techonology*, edited by R. Messier, J. T. Glass, J. E. Butler, and R. Roy (Materials Research Society, Pittsburgh, 1990), p. 857.

[2]W. F. Banholzer and S. Fulghum, in *Proceedings of the International Conference on Optical Science Engineering*, edited by S. Singer (Society of Photo-Optical Instrumentation Engineers Bellingham, 1991), p. 163.

[3]T. R. Anthony, W. F. Banholzer, J. F. Fleischer, L. Wei, P. K. Kuo, R. L. Thomas, and R. W. Pryor, Phys. Rev. B **42**, 1104 (1990).

[4]K. C. Hass, M. A. Tamor, T. R. Anthony, and W. F. Banholzer, Phys. Rev. B **44**, 12 046 (1991).

[5]D. W. Taylor, Phys. Rev. **156**, 1017 (1967).

[6]R. J. Elliott, J. A. Krumhansel, and P. L. Leath, Rev. Mod. Phys. **46**, 465 (1974).

[7]H. Ehrenreich and L. M. Schwartz, in *Solid State Physics*, edited by H. Ehrenreich, F. Seitz, and D. Turnbull (Academic, New York, 1976), Vol. 31, p. 149.

[8]For example, C. Kittel, *Introduction to Solid State Physics*, 5th ed. (Wiley, New York, 1976), Chap. 5, and references therein.

[9]J. W. Bray and T. R. Anthony, Z. Phys. B **84**, 51 (1991).

[10]H. D. Fuchs, C. H. Grein, C. Thomsen, M. Cardona, W. L. Hansen, E. E. Haller, and K. Itoh, Phys. Rev. B **43**, 4835 (1991).

[11]R. Tubino, L. Piseri, and G. Zerbi, J. Chem. Phys. **56**, 1022 (1972).

[12]R. Tubino and J. L. Birman, Phys. Rev. Lett. **35**, 670 (1975); Phys. Rev. B **15**, 5843 (1977).

[13]S. A. Solin and A. K. Ramdas, Phys. Rev. B **1**, 1687 (1970).
[14]M. A. Washington and H. Z. Cummins, Phys. Rev. B **15**, 5840 (1977).
[15]G. Dolling and R. A. Cowley, Proc. Phys. Soc. **88**, 463 (1966).
[16]M. H. Cohen and J. Ruvalds, Phys. Rev. Lett. **23**, 1378 (1969).
[17]K. Uchinokura, T. Sekine, and E. Matsuura, J. Phys. Chem. Solids **35**, 171 (1974).
[18]S. Go, H. Bilz, and M. Cardona, Phys. Rev. Lett. **34**, 580 (1975).
[19]R. Tubino and L. Piseri, Phys. Rev. B **11**, 5145 (1975).
[20]D. Vanderbilt, S. G. Louie, and M. L. Cohen, Phys. Rev. Lett. **53**, 1477 (1984); Phys. Rev. B **33**, 8740 (1986).
[21]C. Z. Wang, C. T. Chan, and K. M. Ho, Solid State Commun. **76**, 483 (1990).
[22]S. Tamura, Phys. Rev. B **27**, 858 (1983).
[23]R. Berman, *Thermal Conduction in Solids* (Clarendon, Oxford, 1976).
[24]P. G. Klemens, Proc. Phys. Soc. A **68**, 1113 (1955).
[25]J. M. Ziman, *Electrons and Phonons* (Oxford University, Press, London, 1963).
[26]D. T. Morelli, G. W. Smith, J. P. Heremans, T. R. Anthony, and W. F. Banholzer, in *Proceedings of the Second International Conference on New Diamond Science and Technology*, edited by R. Messier, J. T. Glass, J. E. Butler, and R. Roy (Materials Research Society, Pitttsburgh, 1990), p. 869.
[27]D. Onn (private communication).
[28]J. R. Olson (private communication).
[29]H. Holloway, K. C. Hass, M. A. Tamor, T. R. Anthony, and W. F. Banholzer, Phys. Rev. B **44**, 7123 (1991).
[30]Equation (2) is analogous to Eq. (14.9b) in Ref. 7, which tends to converge more rapidly than the more common form [Eq. (14.9a)].
[31]P. L. Leath and B. Goodman, Phys. Rev. **181**, 1062 (1969).
[32]K. C. Hass, B. Velický, and H. Ehrenreich, Phys. Rev. B **29**, 3697 (1984).
[33]H. L. McMurry, A. W. Solbrig, J. K. Boyter, and C. Noble, J. Phys. Chem. Solids **28**, 2359 (1967).
[34]R. Tubino and L. Piseri, J. Phys. C **13**, 1197 (1980).
[35]F. Herman, J. Phys. Chem. Solids **8**, 405 (1959).
[36]J. Rath and A. J. Freeman, Phys. Rev. B **11**, 2109 (1975).
[37]J. C. Phillips, Phys. Rev. **104**, 1263 (1956).
[38]A. A. Maradudin, E. W. Montroll, G. H. Weiss, and I. P. Ipatova, *Theory of Lattice Dynamics in the Harmonic Approximation* (Academic, New York, 1971), pp. 150–158.
[39]A. T. Collins, G. Davies, H. Kanda, and G. S. Woods, J. Phys. C **21**, 1363 (1988).
[40]R. M. Chrenko, J. Appl. Phys. **63**, 5873 (1988).
[41]C. J. Chu, M. P. D'Evelyn, R. H. Hauge, and J. L. Margrave, J. Mater. Res. **5**, 2405 (1990).
[42]D. S. Knight and W. B. White, J. Mater. Res. **4**, 385 (1989).
[43]These composition values were determined by a mass-spectroscopic analysis of the combustion products from these diamonds. The slight inaccuracies in the estimated compositions for these samples given in Refs. 4 and 29 do not alter the conclusions of those studies.
[44]The correction is $0.7x$, in cm^{-1}, which is based on the results of Ref. 29 and the Grüneisen parameter of 1.19 for the Raman mode measured by B. J. Parsons, Proc. R. Soc. London A **352**, 297 (1977).
[45]K. C. Hass, H. Ehrenreich, and B. Velický, Phys. Rev. B **27**, 1088 (1983).
[46]C. Z. Wang, C. T. Chan, and K. M. Ho, Phys. Rev. B **42**, 11 276 (1990).
[47]H. Richter, Z. P. Wang, and L. Ley, Solid State Commun. **39**, 625 (1981).
[48]J. W. Ager, D. K. Veirs, and G. M. Rosenblatt, Phys. Rev. B **43**, 6491 (1991).
[49]J. R. McBride, K. C. Hass, and W. H. Weber, Phys. Rev. B **44**, 5016 (1991).
[50]Note that the dashed curve does not correspond exactly to the Bray-Anthony prediction since it does not include any wave-vector dependence of the broadening. In particular, the true Bray-Anthony prediction would exhibit a much sharper upper cutoff and maybe even a sharp 2667-cm^{-1} peak, because the broadening in Ref. 9 is assumed to vanish at the zone center (in disagreement with the observed broadening of the first-order Raman line). The dashed curve is still meaningful, however, since most of the phonons contributing to the main peak near 1250 cm^{-1} do lie near the zone boundaries (cf. Fig. 1) and should experience nearly the maximum broadening in the Bray-Anthony model.
[51]I. M. Lifshitz, Zh. Eksp. Teor. Fiz. **53**, 743 (1967) [Sov. Phys. JETP **26**, 462 (1968)].
[52]J. W. Vandersande, C. B. Vining, and A. Zoltan (unpublished).
[53]I. Pomeranchuk, J. Phys. (Moscow) **6**, 237 (1942).
[54]J. Callaway, Phys. Rev. **113**, 1046 (1959).
[55]R. Berman and M. Martinez, *Diamond Research 1976* (Industrial Diamond Information Bureau, London, 1976), p. 7.
[56]D. T. Morelli, C. P. Beetz, and T. A. Perry, J. Appl. Phys. **64**, 3063 (1988).
[57]T. R. Anthony, J. L. Fleischer, J. R. Olson, and D. G. Cahill, J. Appl. Phys. **69**, 8122 (1991).
[58]Z. Y. Qiu, A. Witek, D. G. Onn, T. R. Anthony, and W. F. Banholzer (unpublished).
[59]R. Berman and J. C. F. Brock, Proc. R. Soc. London A **289**, 46 (1965).
[60]J. M. Ziman, Can. J. Phys. **34**, 1256 (1956).
[61]Note that the mean free path due to isotope scattering in Eq. (2) of Ref. 9 should be reduced by a factor of $(2\pi)^4 \approx 1550$ to be consistent with Eq. (8.6.9) in Ref. 25. Such a reduction implies that even this crude form of Ziman's theory predicts a 26% enhancement in the room-temperature thermal conductivity of diamond from $x = 0.011$ to 0.
[62]H. B. G. Casimir, Physica **5**, 495 (1938).
[63]A similar conclusion appears to have been drawn by V. I. Nepsha, V. R. Grinberg, Yu. A. Klyuyev, A. M. Naletov, and G. R. Bokii, Dokl. Akad. Nauk SSSR **317**, 1 (1991), although there is not sufficient detail given to reproduce their calculations.
[64]For example, T. H. Geballe, Science **250**, 1194 (1990).